Explanation of Pre-Steady-State Kinetics and Decreased Burst Amplitude of HIV-1 Reverse Transcriptase at Sites of Modified DNA Bases with an Additional, Nonproductive Enzyme−DNA−Nucleotide Complex†

Laura Lowe Furge‡ and F. Peter Guengerich*

Department of Biochemistry and Center in Molecular Toxicology, Vanderbilt University School of Medicine, Nashville, Tennessee 37232-0146

Received September 8, 1998; Revised Manuscript Received February 19, 1999

ABSTRACT: The majority of pre-steady-state kinetic investigations with HIV-1 reverse transcriptase (HIV-1 RT) have reported substoichiometric bursts (30−50%) of product formation in the initial reaction cycle. By using quantitative amino acid analysis, we have revised the extinction coefficient of the HIV-1 RT heterodimer and show that normal nucleotide incorporation (canonical four bases) proceeds with quantitative bursts in the first cycle. We have also modeled our previous results with this polymerase, including four situations with 8-oxo-7,8-dihydroguanine (8-oxoGua) moieties in which substoichiometric bursts (2−35%) were observed even after the correction of enzyme concentration by amino acid analysis. These include insertion of dATP opposite template 8-oxoGua, insertion of (deoxy) 8-oxoGua 5′-triphosphate opposite template C, and extension of primers beyond 8-oxoGua−A and 8-oxoGua−C pairs. The "minimal" polymerase mechanism and three others were evaluated using KINSIM and FITSIM methods. The latter three mechanisms involve a conformationally distinct, inactive polymerase−DNA−dNTP complex in equilibrium with the initial ternary complex and a conformationally distinct complex leading to phosphodiester bond formation. All three of the modified mechanisms fit the observed reaction results, but the minimal mechanism did not. Nonfunctional binary complexes (enzyme−DNA) are an alternate explanation (to ternary complexes) in some cases. Finally, DNA trapping experiments indicate that enzyme does not dissociate from the 8-oxoGua-containing DNA substrate prior to phosphodiester bond formation. We conclude that HIV-1 RT is fully active in normal nucleotide incorporation and that substoichiometric bursts with modified systems are well-described by the existence of nonproductive ternary complexes, which can isomerize to productive complexes.

Human immunodeficiency virus type-1 reverse transcriptase (HIV-1 RT)[1] converts the single-stranded viral RNA genome into double-stranded DNA, which is then integrated into the host genome. The mechanism of DNA replication and phosphodiester bond formation employed by HIV-1 RT is the same as that used by other DNA polymerases and has been described (*1*, *2*). This mechanism involves the following steps: the enzyme binds DNA, binds nucleotide, and then undergoes a conformational change prior to bond formation. The conformation then relaxes following bond formation and pyrophosphate release (Figure 1A). Insight into the nature of the conformational change has recently been provided by the crystal structure of HIV-1 RT with duplex DNA and nucleotide and is believed to be related to a change in protein conformation upon substrate binding (*3*). This finding is further supported by X-ray structures of pol β and pol T7 with and without DNA and nucleotide in the active site (*4*−*7*).

It is now established that unusual replication circumstances such as the presence of carcinogen adducts and other modified DNA lesions, secondary structure in the template, inhibitors, misincorporations, and "natural" pause sites may alter polymerase fidelity and catalytic activity. The minimal mechanism is appropriate for normal incorporation reactions, but in replication circumstances described above the minimal mechanism for polymerase activity may be insufficient to describe the experimentally determined data and resulting substoichiometric bursts. These deficiencies have led to an expansion of the minimal mechanism to include additional steps or alternative kinetics (*8*−*16*). One explanation for some of the phenomena is an increased "off" rate (step 7 in Figure 1) for unusual DNA substrates from the polymerases (*13*). However, several groups have shown that there is no simple correlation between dissociation rate and substiochiometric bursts (*8*−*10*, *12*, *14*−*16*). A recent quantitative examination of alternative enzyme kinetics and mechanism has been presented for HIV-1 RT activity on RNA and DNA

† This work was supported in part by United States Public Health Service (USPHS) Grants R35 CA44353 and P30 ES00267. L.L.F. was supported in part by USPHS training Grant T32 ES07028.

* To whom correspondence should be addressed at Department of Biochemistry, Vanderbilt University School of Medicine, Nashville, TN 37232-0146. Tel: (615) 322-2261. Fax: (615) 322-3141. E-mail: guengerich@toxicology.mc.vanderbilt.edu.

‡ Formerly Laura G. Lowe.

[1] Abbreviations: 8-oxoGua, 8-oxo-7,8-dihydroguanine; 8-oxodGTP, (deoxy) 8-oxoGua 5′-triphosphate; Gua or G, guanine; Cyt or C, cytidine; A, adenine; T, thymidine; HIV-1 RT, human immunodeficiency virus-1 reverse transcriptase; KF^+, *Escherichia coli* polymerase I (Klenow fragment) exo^+; KF^-, *Escherichia coli* polymerase I (Klenow fragment) exo^-; pol β, mammalian DNA polymerase β; pol $T4^-$, T4 DNA polymerase exo^-; pol $T7^-$, T7 DNA polymerase exo^-.

10.1021/bi982163u CCC: $18.00
Published on Web 03/25/1999

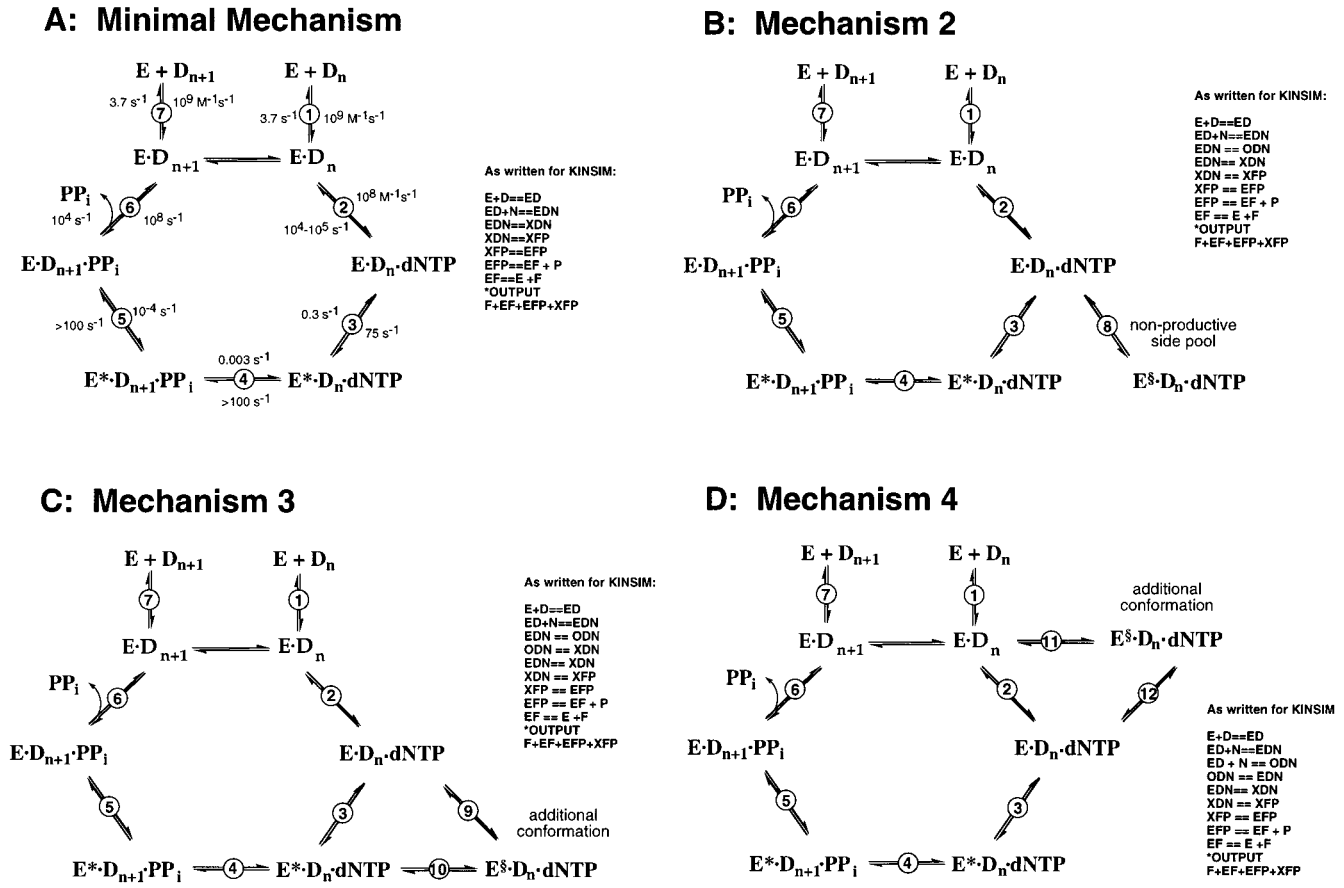

FIGURE 1: Kinetic mechanisms for DNA polymerases. Individual steps are numbered: E = polymerase, D_n = DNA, E* = conformational change in polymerase, and D_{n+1} = DNA extended by one base. To the right of each schematic, the mechanism is shown as written in Simple Text and used for kinetic simulations using KINSIM and FITSIM: N = nucleotide triphosphate, X = conformational change in polymerase, O = additional conformational state of ternary complex, F = DNA extended by one base, and P = pyrophosphate. (A) Minimal kinetic mechanism. Forward and reverse rate constants for each step are given on the basis of simulations of pre-steady-state nucleotide incorporation reactions with nonmodified substrates. (B) Kinetic mechanism 1. An additional, nonproductive side-pool of enzyme−DNA−nucleotide is formed. (C) Kinetic mechanism 3. An additional enzyme−DNA−nucleotide state is formed which is catalytically competent, but not kinetically favorable. (D) Kinetic mechanism 4. At nucleotide binding, two conformations of ternary complex are formed, only one of which is catalytically competent.

Table 1: Quantitative Amino Acid Analysis of HIV-1 RT[a]

amino acid	nmol recovered	nmol expected
Asp	330	662
Ser	157	375
Gly	321	431
His	133	136
Arg	130	327
Thr	272	479
Ala	284	279
Cys	37	64
Tyr	105	335
Val	290	503
Met	59	120
Lys	387	814
Ile	252	535
Leu	374	678
Phe	116	176
Pro	258	599
total	3505	6513

[a] See Experimental Procedures for details of analysis.

substrates with secondary structure in a series of papers by Suo and Johnson (*8*−*10*, *15*). They show that pausing is due to a reduced burst amplitude without reduced burst rate and conclude that the cause is partial nonproductive DNA or RNA substrate binding and not enzyme dissociation. Likewise, Suo et al. (*14*) have shown that nucleotide addition by HIV-1 RT in the presence of a single cis-platin DNA intrastrand cross-link, an adduct that alters the structure of the double helix, proceeds via productive and nonproductive enzyme−DNA complexes which isomerize to productive forms. Thus, there is considerable precedence for the formation of nonproductive enzyme−substrate complexes, at least with seriously distorted DNA substrates.

We have observed substoichiometric burst amplitudes during pre-steady-state nucleotide addition by HIV-1 RT in the presence of 8-oxoGua in template DNA or as the incoming nucleotide (*17*, *18*). Substoichiometric bursts in unusual replication circumstances involving DNA adducts are not limited to HIV-1 RT. Substoichiometric bursts have also been observed for the incorporation of dTTP opposite the adenine base analogue 2-aminopurine by KF^-, pol $T4^-$ and pol β (*19*−*21*). In addition, incorporation of T and C opposite O^6-methylGua by KF^+ and extension of resulting O^6-methylGua−T or −C base pairs displays substoichiometric burst kinetics (*22*), as does C incorporation opposite a cis-platin intrastrand cross-link by pol $T7^-$ (and HIV-1 RT) (*14*).

The focus of our work has been 8-oxoGua, the quantitatively most important DNA adduct formed from reactive

oxygen species. 8-OxoGua is a small, but mutagenic, DNA adduct and does not cause significant distortion of the double helix (*23*−*25*). Polymerase studies to date have shown that 8-oxoGua base pairs with both the correct pairing partner, C, and the mutagenic pairing partner, A (*17*, *26*−*29*). Polymerases examined to date prefer to incorporate C opposite template 8-oxoGua, with A being inserted when C is not. HIV-1 RT is much more efficient at inserting A opposite 8-oxoGua (*17*). Furthermore, polymerase studies have shown preferential extension of terminal 8-oxoGua−A base pairs rather than the 8-oxoGua−C "correct" pair (*17*, *26*−*28*, *30*, *31*). Our results, and those of others (*1*, *8*, *12*, *32*−*34*), were fit to a general burst equation that is independent of mechanism, and full simulations to the minimal mechanism could only fit the results when artificially lowered enzyme concentrations were substituted (*17*, *18*).

In the present work we used a computer simulation to model our HIV-1 RT and 8-oxoGua adduct results. Expansion of the minimal mechanism is required to describe these substoichiometric bursts. The alternative path is postulated to include the formation of nonproductive enzyme−DNA−nucleotide pools. These results, taken along with recent reports by Suo and Johnson (*8*−*10*, *14*, *15*), may have bearing on physical studies directed toward understanding DNA polymerases and their interactions with modified DNA substrates.

EXPERIMENTAL PROCEDURES

Quantitative Amino Acid Analysis. Aliquots from three separate preparations of HIV-1 RT from this laboratory (*17*) were submitted for quantitative amino acid analysis to the Vanderbilt Protein Chemistry Facility. The molar content of each preparation was estimated using $\epsilon_{280} = 261\ mM^{-1}\ cm^{-1}$ (*2*) for the heterodimer prior to submission of the samples. The samples were hydrolyzed for 24 h under vacuum at 110 °C in 6 N HCl and then analyzed as 6-aminoquinolyl-*N*-hydroxysuccinimidyl carbamate derivatives by HPLC using a Waters AccQ-Tag System (Milford, MA).

Computer Simulations. Simulations modeling the observed kinetic curves for nucleotide incorporation were done by mathematical analysis using HopKINSIM version 1.7 for Macintosh and KINSIM (version April 3, 1997) for PC, obtained from Prof. C. Frieden (Washington University, St. Louis, MO) (*35*−*37*). Regression analysis was done using the companion program FITSIM (*38*). HopKINSIM was run on a Macintosh Power PC 9600 computer (Apple Computer Inc., Cupertino, CA) equipped with SoftwareFPU version 3.03 (John Neil & Associates, Cupertino, CA). KINSIM and FITSIM were run in DOS version 7.0 on an IBM PC. The graphs shown were generated in KaleidaGraph version 3.0.5 (Synergy Software, Reading, PA).

Calculation of the pre-steady-state time course for nucleotide incorporation by polymerases can be achieved using the computer kinetic modeling system KINSIM. With this program, a mechanism for the enzymatic reaction is written in a text editor using simple notation (Figure 1). In the mechanism, the double equal sign (==) defines a reversible step governed by both forward and reverse rate constants. A single equals sign (=) defines a step governed by a dissociation constant. The output equation is indicated at the end of the mechanism following the *OUTPUT notation. In the case of rapid-quench gel-based extension assays, all products formed at and after phosphodiester bond formation contribute to the overall product formation and are, therefore, all included in the output equation (Figure 1). Once a mechanism has been set up, rate constants are supplied for each step on the basis of experimentally determined values and assumptions. With the mechanism and rate constants defined, one supplies the starting reactant concentrations and then runs the simulation of the mechanism with the given rate constants and reactant concentrations. The simulated curve(s) is (are) then compared to the experimental data points to judge how closely the set of rate constants simulate the experimental data. Adjustments to initial rate constant entries are then made until the simulated curve(s) is (are) close to the experimental data. At this point, the iterative nonlinear regression analysis program FITSIM is used to predict how well the mechanism and set of rate constants describe the experimental data. By using this system, one is able to rapidly and efficiently test multiple mechanisms.

Rapid-Quench Experiments with Excess DNA Trap. Experiments were carried out in a rapid-quench apparatus as previously described (*8*, *17*) (primer sequence, 5′-GCCTCGAGCCGCAGACGCAG; template sequence, 3′-CGGAGCTCGGCGTCTGCGTCXCTCCTGCGGCT, where X = 8-oxoGua). In the DNA trap experiments, a solution of HIV-1 RT (50 nM) was incubated with 8-oxoGua-containing 36-mer−24-mer primer complex (100 nM) (primer labeled with ^{32}P in the usual way) and then mixed with dATP (400 μM), unlabeled Gua-containing 24/36-mer (5 μM), and a Mg^{2+}-containing buffer (12.5 mM Mg^{2+}). For comparison, experiments without excess unlabeled DNA were also performed. The reactions were quenched with 0.3 M EDTA at time intervals ranging from 25 ms to 75 s. DNA products were quantitated as described (*17*). The biphasic kinetic data from experiments with DNA trap were fitted with a double-exponential equation: $[\text{product}] = E_0A_1[1 - \exp(-k_1t)] + E_0A_2[1 - \exp(-k_2t)]$, where E_0 represents the total enzyme concentration, A_1 the fast-phase enzyme amplitude, k_1 the observed fast-phase rate, A_2 the slow-phase enzyme amplitude, and k_2 the observed slow-phase rate (*8*).

RESULTS AND DISCUSSION

Quantitative Amino Acid Analysis of HIV-1 RT. In our initial studies with HIV-1 RT and incorporations involving the four canonical bases, we noticed that our preparation of HIV-1 RT only showed ∼50% activity in active-site titration experiments (*17*). Several other groups using the same and different overexpression systems and purification schemes as ours also reported 30−50% activity based on active-site titration experiments (*2*, *11*, *32*−*34*, *39*, *40*). Quantitative amino acid analysis of our HIV-1 RT preparations showed only ∼50% of the expected recovery of protein based on UV measurement and $\epsilon_{280} = 261\ mM^{-1}\ cm^{-1}$ (Table 1). The same results were obtained when the amino acid analysis was calculated by adding measured weights of individual amino acids, and nearly identical results were obtained with three separate analyses. Thus, the revised ϵ_{280} for the heterodimer is $520\ mM^{-1}\ cm^{-1}$, and our preparation of HIV-1 RT is nearly 100% active in active-site titrations (all concentrations of HIV-1 RT reported in this paper are based on $\epsilon_{280} = 520\ mM^{-1}\ cm^{-1}$). This result probably also explains many of the partial bursts reported by others in the literature

for HIV-1 RT in normal nucleotide incorporation. Furthermore, Jaju et al. (*16*) observed proportional burst amplitudes (using conventional mixing experiment protocols) when the concentration of HIV-1 RT was determined by amino acid analysis (no extinction coefficient was reported).

Fitting of Kinetic Results to Polymerase Minimal Mechanism. The program KINSIM has been used by many groups to analyze the minimal mechanism of polymerases during normal incorporation reactions and misincorporation reactions involving normal bases (*2*, *12*, *16*, *17*, *21*, *27*, *41*−*46*). For the biphasic incorporation of dCTP (220 μM) opposite template Gua (102 nM DNA) by HIV-1 RT (14 nM),[2] the simulation with the minimal mechanism and rate constants shown (Figure 1A) and the indicated starting reactant concentrations yields a reasonable fit to the experimental data (Figure 2A) (*30*). For simplicity, the data for only a single saturating concentration of nucleotide is shown, but the mechanism and rate constants apply at all concentrations of nucleotide used in previous studies (*17*). The burst amplitude, approximately 13 nM, is nearly stoichiometric with the starting concentration of HIV-1 RT. The stoichiometric relationship between the burst amplitude and concentration of enzyme is a hallmark feature of pre-steady-state DNA polymerase extension assays and reflects the concentration of active enzyme−DNA complex when the reaction is initiated by the addition of nucleotide and Mg^{2+}.

Although the minimal mechanism describes the burst kinetics for a normal incorporation reaction well, it fails to closely simulate the burst kinetics for incorporation of dATP (220 μM) opposite the DNA adduct 8-oxoGua (102 nM DNA) by HIV-1 RT (32 nM) (Figure 2B). In this case, the burst amplitude is only ~16% of the expected amplitude and is said to be substoichiometric relative to the concentration of active enzyme, even after correction of the enzyme concentration by quantitative amino acid analysis. Adjustment of the rate constants does not provide a more reasonable fit, and several different attempts to achieve a desirable fit are shown (Figure 2B). However, a reasonable fit can be achieved if the starting concentration of HIV-1 RT is given as ~5 nM (the burst amplitude) rather than the actual 32 nM used experimentally (results not shown). Thus, the minimal mechanism is insufficient to describe the observed substoichiometric burst.

Substoichiometric bursts with HIV-1 RT have also been described in the literature for the misincorporation of nucleotides, for incorporation at pause sites generated by secondary template structure or "natural" sequences, for incorporation of nucleotides in the presence of nonnucleoside inhibitors, and for incorporation opposite DNA adducts (*2*, *8*, *11*−*15*, *33*, *34*). In each of these cases, models were proposed to explain this phenomenon including expansion of the minimal mechanism to include additional conformations either of enzyme−DNA or of enzyme−DNA−nucleotide complexes. All of the proposed possibilities can be rapidly checked for agreement with experimental data using the kinetic modeling program KINSIM. It is imperative to note, however, that a good fit of the experimental data does not prove a mechanism to be correct. At best, fitting provides support for the proposed mechanism and can be used to rule out some possible mechanisms.

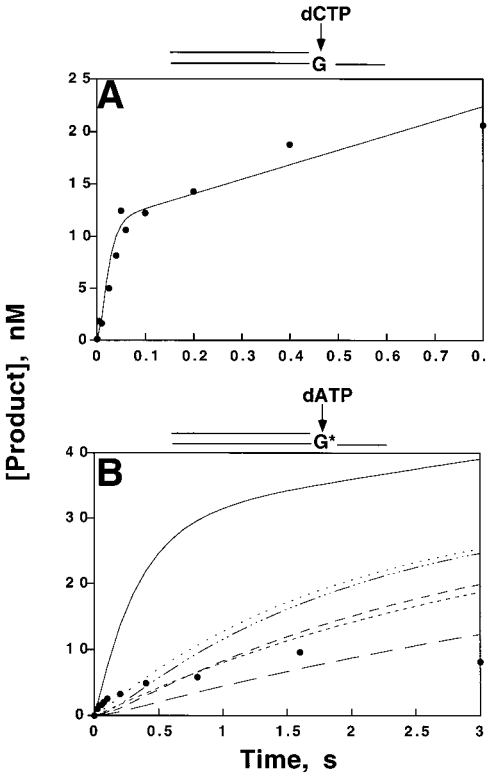

FIGURE 2: Comparison of simulations to the minimal mechanism of pre-steady-state kinetics showing stoichiometric and substoichiometric burst amplitudes relative to the concentration of active polymerase. (A) The solid circles represent the incorporation of the correct nucleotide, dCTP (220 μM), opposite Gua (DNA = 102 nM) by HIV-1 RT (14 nM) as shown schematically above the graph. Rapid-quench experiments were initiated by the mixing of dCTP in a Mg^{2+}-containing buffer with a preincubated solution of HIV-1 RT and DNA and were quenched at the specified times with 0.3 M EDTA (*17*). The solid line represents the simulation of the results by the minimal mechanism and rate constants shown in Figure 1A. (B) The solid circles represent the incorporation of dATP (220 μM) opposite 8-oxoGua (DNA = 102 nM) by HIV-1 RT (32 nM) as shown schematically above the graph where G* is 8-oxoGua. Rapid-quench experiments were initiated by the mixing of dATP in a Mg^{2+}-containing buffer with a preincubated solution of HIV-1 RT and 8-oxoGua-containing DNA and were quenched at the specified times with 0.3 M EDTA (*17*). The lines represent examples of the unsatisfactory fits of the results by the minimal mechanism. Variations from the rate parameters shown in Figure 1A are as follows: (—) $k_{+3} = 10\ s^{-1}$, $k_{+4} = 10^3\ s^{-1}$, $k_{+7} = 0.1\ s^{-1}$; (•••) $k_{+3} = 3\ s^{-1}$, $k_{+4} = 10^2\ s^{-1}$; (—•••—) $k_{+3} = 3\ s^{-1}$, $k_{+4} = 10\ s^{-1}$; (— — —) $k_{+3} = 2\ s^{-1}$, $k_{+4} = 10\ s^{-1}$; (---) $k_{+3} = 1\ s^{-1}$, $k_{+4} = 10^2\ s^{-1}$; (— — —) $k_{+3} = 1\ s^{-1}$, $k_{+4} = 10\ s^{-1}$. (Not shown: variations in k_{-3} and k_{-4} and other combinations that did not yield better fits).

Possible Mechanisms To Describe Substoichiometric Bursts: Insertion of dATP Opposite Template 8-OxoGua. A mechanism that has been proposed by several groups, including our own, to explain substoichiometric bursts includes an additional ternary complex of enzyme−DNA−nucleotide that is not catalytically competent (Figure 1B). The mechanism is designated mechanism 2.

A number of binding studies have shown that polymerases bind a variety of DNA substrates, including those with mismatched termini, blunt ends, and secondary template structure, with affinity similar to that of nonmodified DNA

[2] The K_d^{dNTP} and k_{pol} values for all reaction sets discussed in this manuscript have been previously determined (*17*, *18*) and are as follows: for (indicated as nucleotide/template base pairing) dCTP/Gua, $K_d^{dCTP} = 4.1 \pm 1.8\ \mu M$, $k_{pol} = 42 \pm 5\ s^{-1}$; for dATP/8-oxoGua, $K_d^{dATP} = 10 \pm 6\ \mu M$, $k_{pol} = 1.3 \pm 0.2\ s^{-1}$; and for 8-oxodGTP/Cyt, $K_d^{8-oxodGTP} = 2.3 \pm 1.0$ mM, $k_{pol} = 15\ s^{-1}$.

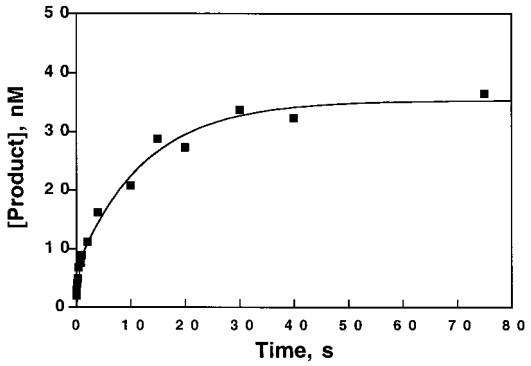

FIGURE 3: DNA trapping experiment. The incorporation of dATP opposite 8-oxoGua was examined at 37 °C as described (*8*). A solution of HIV-1 RT (50 nM) was incubated with 8-oxoGua-containing 36-mer−24-mer primer complex (100 nM) and then mixed with dATP (400 μM), Mg^{2+} (12.5 mM), and excess unlabeled Gua-containing 36-mer−24-mer primer complex (5 μM) (■). The reactions were quenched by the addition of 0.3 M EDTA at time intervals from 25 ms to 75 s. The data were fitted to a double exponential with $k_1 = 9.2 \pm 3.8\ s^{-1}$ and $k_2 = 0.08 \pm 0.01\ s^{-1}$.

(*8*, *17*, *47*). Although such results do not confirm an ability to move forward in the catalytic cycle, they do support a ground state binding of DNA that is largely independent of DNA content and structure.[3] In DNA trapping experiments, the incorporation of dATP opposite 8-oxoGua followed biphasic kinetics in the presence (and absence) of unlabeled DNA (Figure 3). The two phases, both first-order, are separated by 2 orders of magnitude. In the absence of the trap, the incorporation in the second exponential phase is slightly greater, and then the reaction proceeds into the usual steady state (results not shown). With the trap DNA present, then, the initial burst corresponds to 13% incorporation, followed by a reaction (thought to involve isomerization to an active complex), and yields another 55% incorporation. This result, similar to that reported with RNA and DNA containing strong secondary structure by Suo and Johnson (*8*, *15*) and with cis-platin-adducted DNA by the same group (*14*), indicates that the formation of product occurs largely without enzyme dissociation from the duplex DNA. Furthermore, both product curves could be fit with mechanism 2 and the rate constants shown in Table 2, which were developed on the basis of the rates estimated in Figure 3 and improved by FITSIM modeling.

Experimental results for the incorporation of saturating and subsaturating concentrations of dATP opposite template 8-oxoGua by HIV-1 RT are fit well by this mechanism and the rate constants indicated in Table 2 (Figure 4). All other rate constants are the same as those shown in Figure 1A for the simulation of a normal incorporation (Figure 2A). In mechanism 2, the value of k_{-8} controls the rate of the steady-state phase. The greater the value of k_{-8}, the larger the slope of the second, slower phase. The rate of the burst phase is controlled by the value of k_{+3}. The level of the substoichiometric burst is controlled by k_{+8} such that the greater the value of k_{+8}, the lower the burst amplitude of the curve.

In mechanism 3, the additional conformational complex of enzyme−DNA−nucleotide may move forward in the catalytic cycle to a conformation competent for bond formation or may move back in the cycle to the initial nucleotide ground-state binding conformation (Figure 1C). At the step of nucleotide binding, the formation of productive and nonproductive ternary complexes may occur as described in mechanism 4 (Figure 1D). The incorporation of dATP opposite template 8-oxoGua by HIV-1 RT is also fit well by both mechanisms 3 and 4 (results not shown). Since the experimental data is not sufficient to distinguish the three alternative mechanisms and because they are similar, for simplicity this manuscript will focus on results obtained with mechanism 2.

Another mechanism to describe substoichiometric bursts is the existence of two enzyme−DNA binary complexes, only one of which is able to bind dNTP and is catalytically competent (mechanism not shown) (*8*, *11*). We also used this mechanism for kinetic simulations and were able to achieve a reasonable fit to our data (results not shown). This mechanism can describe some substoichiometric bursts well, although it cannot be invoked for cases with normal DNA and modified nucleotide (vide infra). Although the mechanism leading to nonproductive enzyme−substrate complex need not be the same for cases when 8-oxoGua is in the template and when it is in the incoming nucleotide, both mechanisms may still result from a nonproductive enzyme−DNA−nucleotide complex. In one case the DNA may prove to be the blocking agent while in the other the nucleotide may be the hindrance to progression in the catalytic cycle. Also, in cases where DNA is the blocking substrate, nucleotide binding may not necessarily be inhibited in all cases. A mechanism involving a nonproductive ternary complex for the case of HIV-1 RT and 8-oxoGua is further supported in that the ground-state nucleotide binding determined by the value of K_d^{dNTP} is <2-fold different between binding dCTP when Gua is in the template and binding dATP when 8-oxoGua is in the template (4 ± 2 vs 10 ± 6 μM) (*17*). The combination of these findings and mechanisms suggests that a principal pathway to nonproductive complexes may involve a nonproductive ternary complex in addition to a nonproductive binary complex of enzyme−DNA in some cases (i.e., DNA distorting adducts and cases where K_d^{dNTP} may vary by manyfold).

Insertion of 8-oxodGTP Opposite Template Cyt by HIV-1 RT. The pre-steady-state addition of 8-oxodGTP (5 mM) opposite template Cyt (100 nM duplex DNA) by HIV-1 RT (36 nM) shows a substoichiometric burst of ~5% (Figure 5) (*18*). As opposed to the system discussed in the above section, the DNA substrate is not modified in this case; only the nucleotide is modified. When the minimal mechanism (1) is applied to these data, no reasonable fit is obtained with any combination of rate constants (Figure 5). The fit with the minimal mechanism shown is only one of many unsatisfactory fits (Figure 5). However, all three of the alternative mechanisms (2, 3, or 4) provide satisfactory fits to the data using the rate constants shown in Table 2. Thus, the alternative mechanisms apply when the unusual replication circumstance is due to a modified nucleotide. Furthermore, in this case it is not reasonable to invoke a model of an altered enzyme−DNA binary complex incapable of catalysis as an explanation for the substoichiometric burst, because the DNA is normal and yields a full burst with the normal dNTP (Figure 2A).

[3] As previously determined, the affinity of HIV-1 RT for adduct-containing DNA is within the generally accepted K_d^{DNA} range [10−30 nM (*48*)] and does not differ greatly from the K_d^{DNA} for nonadducted DNA (*17*, *18*).

Table 2: Pre-Steady-State Rate Constants[a]

		dNTP/template pairing[b]			
mechanism 2	*k*	dATP−8-oxoGua	8-oxodGTP−Cyt	dGTP/Cyt after 8-oxoGua−A	dGTP/Cyt after 8-oxoGua−C
EDN ⇌ XDN	+3	26 ± 2	24 ± 1	41 ± 2	21 ± 3
EDN ⇌ ODN	+8	136 ± 12	572 ± 15	79 ± 13	645 ± 22
	−8	0.5 ± 0.1	3.9 ± 0.4	4 ± 1	9 ± 2

[a] All values are expressed in units of s^{-1}. Indicated errors were estimated using FITSIM. [b] See refs *17* and *18*.

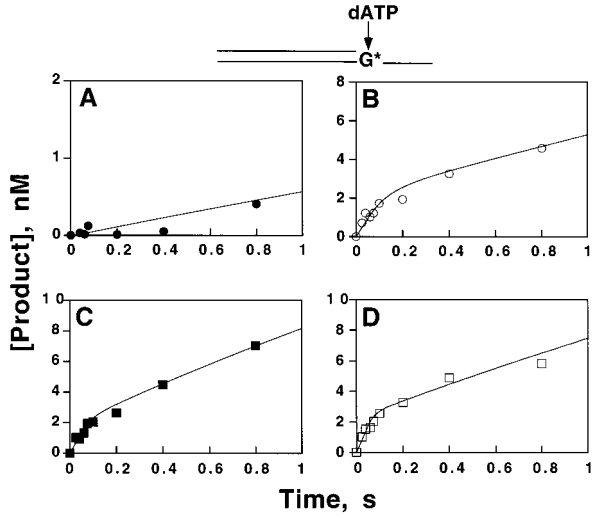

FIGURE 4: Simulations using mechanism 2 with varying concentrations of dATP. The experimental results are from ref *17*. Briefly, a preincubated solution of HIV-1 RT (32 nM) and 8-oxoGua-modified DNA (102 nM) was mixed with increasing concentrations of dATP (1 μM, ●; 28 μM, ○; 55 μM, ■; and 220 μM, □) in a Mg^{2+}-containing buffer as shown schematically above the graph where G* is 8-oxoGua. The reactions were stopped with 0.3 M EDTA in a rapid-quench apparatus at the indicated times, and the concentration of product was determined by gel analysis as described previously (*17*). The results for each concentration are shown in separate panels. The solid line in each panel represents the fit with mechanism 2 to the results and the rate constants shown in Table 2. (A) 1 μM dATP, (B) 28 μM dATP, (C) 55 μM dATP, (D) 220 μM dATP.

Next Correct Base Addition Following an 8-oxoGua−A or an 8-oxoGua−C Base Pair. Although incorporation of the next correct base following a mismatch occurs at a greatly reduced rate compared to incorporation after a normal base pair, the reduced rate is attributable to a kinetic barrier to extension rather than to polymerase difficulty in binding mismatched termini (*30*, *47*). In the case of 8-oxoGua adduct pairs, the rate of extension of 8-oxoGua−A base pair is greater than that for extension of 8-oxoGua−C with all polymerases examined when 8-oxoGua is in the template strand (*17*, *26*, *27*). Extension of both base pairs by HIV-1 RT shows substoichiometric burst kinetics with ∼30% and ∼5% burst amplitudes for extension of 8-oxoGua−A and 8-oxoGua−C, respectively (Figure 6) (*17*). When the data is fit with the minimal mechanism (1), a pronounced lag in product formation and an unsatisfactory fit are observed (Figure 6). This is in contrast to the fits observed with the three alternative mechanisms (2, 3, or 4), which closely simulate the experimental data using the rate constants in Table 2. The results show that the alternative mechanisms also apply to substoichiometric bursts observed in the next correct base addition reactions.

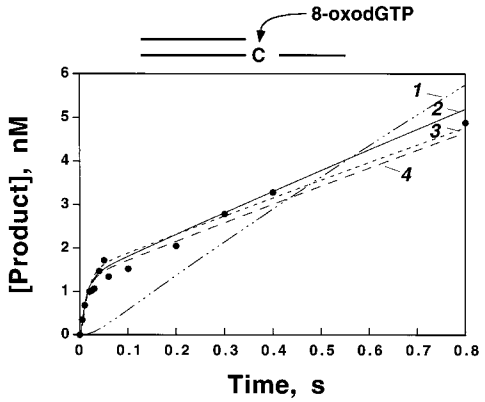

FIGURE 5: Incorporation of 8-oxodGTP opposite template Cyt by HIV-1 RT. The solid circles are pre-steady-state data from ref *18* for the incorporation of 8-oxodGTP (5 mM) opposite template Cyt (100 nM duplex DNA) by HIV-1 RT (36 nM) as shown schematically above the graph. Reactions were initiated by the mixing of 8-oxodGTP in a Mg^{2+}-containing buffer with a preincubated solution of HIV-1 RT and DNA and were quenched at the specified times with 0.3 M EDTA. Simulation of the results by the minimal mechanism 1 (−···−), mechanism 2 (—), mechanism 3 (---), and mechanism 4 (− − −) are shown.

Conclusions. Nonproductive substrate binding by HIV-1 RT leads to reduced burst amplitudes in unusual replication situations such as those encountered with DNA adducts, DNA/RNA secondary structure, and others (*2*, *8*, *9*, *12*−*15*, *32*−*34*, *49*). Mechanisms of nonproductive substrate binding involving ternary complexes that may result in some of these circumstances are given in Figure 1. Mechanism 2 is the least complicated of the three, but it is not clear where the nonproductive complex originates, that is, nonproductive enzyme−DNA or enzyme−DNA−nucleotide complex.

By using the values in Table 2 for the simulation of dATP incorporation opposite 8-oxoGua with mechanism 2, we predicted a burst amplitude of ∼16% of the maximum amplitude on the basis of the following relationship: burst amplitude $\approx k_{+3}/(k_{+3} + k_{+8})$(100% of the theoretical maximum burst) (i.e., competition of reactions 3 and 8). The results show ∼16% burst (∼5 nM burst amplitude/32 nM HIV-1 RT), in good agreement between the simulations and observed results. Also, when applied to the other three scenarios (8-oxodGTP opposite Cyt and dGTP after 8-oxoGua−A and 8-oxoGua−C), the same agreement between predicted and actual burst amplitudes is observed. These calculations support the validity of mechanism 2 as a model to describe substoichiometric burst kinetics encountered in various settings with modified DNA bases. Thus, when polymerases (at least HIV-1 RT) encounter such entities, multiple ternary (polymerase-DNA-dNTP) complexes can be found. Three distinct kinetic phases can be observed: (i) a rapid burst involving a fast conformational change and phosphodiester bond formation, analogous to incorporation

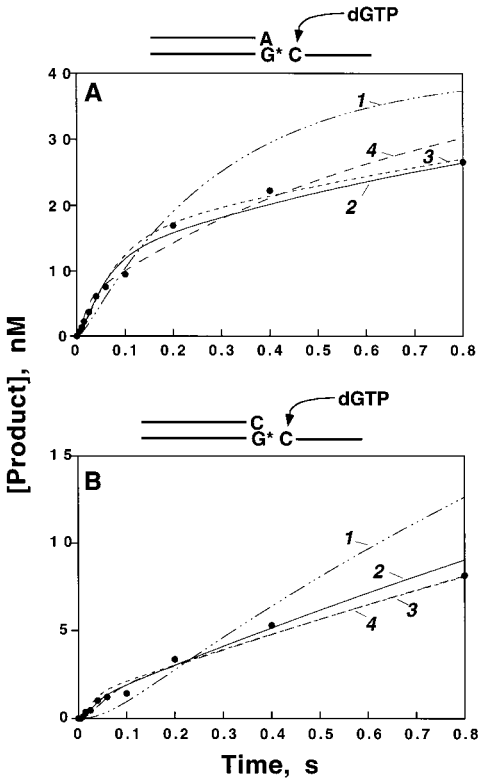

FIGURE 6: Incorporation of the next correct nucleotide after 8-oxoGua−A and 8-oxoGua−C base pairs by HIV-1 RT. The solid circles are pre-steady-state results from ref *17* for the incorporation of dGTP (220 μM) opposite template Cyt in duplex DNA (102 nM) by HIV-1 RT (40 nM) as shown schematically above the graph where G* is 8-oxoGua. Rapid-quench experiments were initiated by the mixing of dGTP in a Mg^{2+}-containing buffer with a preincubated solution of HIV-1 RT and DNA and were quenched at the specified times with 0.3 M EDTA (*17*). (A) Extension past 8-oxoGua−A base pair by incorporation of dGTP. (B) Extension past 8-oxoGua−C base pair by incorporation of dGTP. Simulation to the results by the minimal mechanism 1 (−•••−), mechanism 2 (−), mechanism 3 (---), and mechanism 4 (− − −) is shown.

with normal DNA/dNTPs and at a similar rate (Figure 3); (ii) a slower first-order reaction involving conversion of inactive ternary complex(es) to active complex, followed by phosphodiester bond formation (Figure 3); and (iii) dissociation of the ternary complex and binding of DNA for the next step, at least with short pieces of DNA, to yield the observed steady-state reaction. Depending on the system, steps (ii) and (iii) may compete and thus lower the yield of product. The sensitivity of proposed step (ii) to other DNA modifications is the subject of further research in this laboratory.

An evaluation of the equilibrium constants (K_{eq}) determined from the rate constants used in the simulation of dATP incorporation opposite 8-oxoGua with mechanism 2 shows that the equilibrium for the reaction is slightly in favor of the nonproductive side-pool (Figure 7 and Table 2). The equilibrium may shift, however, in either direction depending on the value of the more flexible parameter k_{-3}. We established (using KINSIM) an upper limit for the value of k_{-3} at 10 s^{-1} and a lower limit of 10^{-6} s^{-1} [we have shown the value 0.3 s^{-1} as estimated by Hsieh et al. (*1*) for HIV-1 RT as an approximation of the true value (Figures 1A and 7)], so the equilibrium may vary considerably. Therefore, physical studies aimed at understanding polymerases in unusual replication circumstances must take into consider-

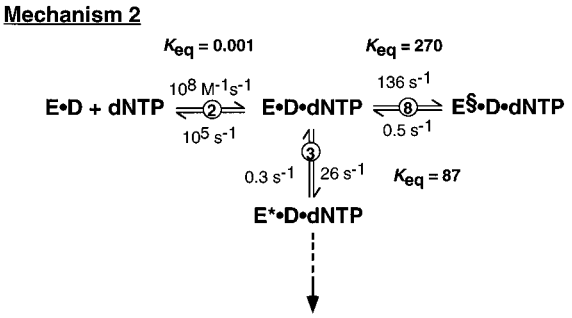

FIGURE 7: Equilibrium constants based on mechanism 2 for the insertion of dATP opposite 8-oxoGua. Forward and reverse rate constants are as shown in Table 2. The value of k_{-3} is from Hsieh et al. (*1*). See text for discussion.

ation the possible large presence of alternative conformations and side-pools with varying physical characteristics. Furthermore, studies using dideoxy-terminated primers (not capable of proceeding past step 3) may receive considerable contribution from a nonproductive side-pool.

Overall, the satisfactory kinetic simulations of the nucleotide addition reactions with mechanisms 2, 3, and 4 are strongly indicative of some type of nonproductive pool of ternary enzyme−DNA−nucleotide complex to explain substoichiometric bursts related to replication involving 8-oxoGua in the template or as the incoming nucleotide. Suo and Johnson have already shown that, with RNA and DNA hairpin structures, pausing during replication is due to the presence of nonproductive enzyme−DNA complexes which must isomerize to a catalytically competent form before continuing in the polymerase cycle (*8*−*10*, *15*). They found the same to be true for replication at cis-platin DNA intrastrand cross-links (*14*). Thus, as replication circumstances are varied, nonproductive conformations may arise in the enzyme, DNA, or nucleotide and contribute to the formation of nonproductive ternary and/or binary complexes.

In conclusion, we have shown by quantitative amino acid analysis that normal nucleotide incorporation by HIV-1 RT proceeds with stoichiometric bursts in the first cycle and, using kinetic modeling, that pre-steady-state substoichiometric bursts with substrates that are not highly distorted compared to normal substrates are better described by the presence of nonproductive ternary complexes than by the minimal mechanism alone. Further work will be required to discriminate among the possibilities and to characterize them. Finally, these findings may explain substoichiometric bursts observed during incorporation reactions by polymerases other than HIV-1 RT.

ACKNOWLEDGMENT

We thank E. Howard for the quantitative amino acid analysis, Prof. C. Frieden for supplying the KINSIM and FITSIM programs, Dr. H. J. Einolf (*18*) for providing some of the data used in the analysis, and Drs. G. P. Miller and W. W. Johnson for comments on the modeling and the manuscript.

REFERENCES

1. Hsieh, J.-C., Zinnen, S., and Modrich, P. (1993) *J. Biol. Chem. 268*, 24607−24613.

2. Kati, W. M., Johnson, K. A., Jerva, L. F., and Anderson, K. S. (1992) *J. Biol. Chem. 267*, 25988−25997.
3. Huang, H., Chopra, R., Verdine, G. L., and Harrison, S. C. (1998) *Science 282*, 1669−1675.
4. Sawaya, M. R., Prasad, R., Wilson, S. H., Kraut, J., and Pelletier, H. (1997) *Biochemistry 36*, 11205−11215.
5. Pelletier, H., Sawaya, M. R., Wolfle, W., Wilson, S. H., and Kraut, J. (1996) *Biochemistry 35*, 12742−12761.
6. Doublié, S., Tabor, S., Long, A. M., Richardson, C. C., and Ellenberger, T. (1998) *Nature 391*, 251−257.
7. Steitz, T. A. (1998) *Nature 391*, 231−232.
8. Suo, Z., and Johnson, K. A. (1997) *Biochemistry 36*, 12459−12467.
9. Suo, Z., and Johnson, K. A. (1997) *Biochemistry 36*, 14778−14785.
10. Suo, Z., and Johnson, K. A. (1997) *Biochemistry 36*, 12468−12476.
11. Pop, M. P., and Biebricher, C. K. (1996) *Biochemistry 35*, 5054−5062.
12. Zinnen, S., Hsieh, J. C., and Modrich, P. (1994) *J. Biol. Chem. 269*, 24195−24202.
13. Klarmann, G. J., Schauber, C. A., and Preston, B. D. (1993) *J. Biol. Chem. 268*, 9793−9802.
14. Suo, Z., Lippard, S. J., and Johnson, K. A. (1999) *Biochemistry 38*, 715−726.
15. Suo, Z., and Johnson, K. A. (1998) *J. Biol. Chem. 273*, 27259−27267.
16. Jaju, M., Beard, W. A., and Wilson, S. H. (1995) *J. Biol. Chem. 270*, 9740−9747.
17. Furge, L. L., and Guengerich, F. P. (1997) *Biochemistry 36*, 6475−6487.
18. Einolf, H. J., Schnetz-Boutaud, N., and Guengerich, F. P. (1998) *Biochemistry 37*, 13300−13312.
19. Frey, M. W., Sowers, L. C., Millar, D. P., and Benkovic, S. J. (1995) *Biochemistry 34*, 9185−9192.
20. Zhong, X., Patel, S. S., Werneburg, B. G., and Tsai, M. D. (1997) *Biochemistry 36*, 11891−11900.
21. Eger, B. T., and Benkovic, S. J. (1992) *Biochemistry 31*, 9227−9236.
22. Tan, H. B., Swann, P. F., and Chance, E. M. (1994) *Biochemistry 33*, 5335−5346.
23. Lipscomb, L. A., Peek, M. E., Morningstar, M. L., Verghis, S. M., Miller, E. M., Rich, A., Essigmann, J. M., and Williams, L. D. (1995) *Proc. Natl. Acad. Sci. U.S.A. 92*, 719−723.
24. Kouchakdjian, M., Bodepudi, V., Shibutani, S., Eisenberg, M., Johnson, F., Grollman, A. P., and Patel, D. J. (1991) *Biochemistry 30*, 1403−1412.
25. McAuley-Hecht, K. E., Leonard, G. A., Gibson, N. J., Thomson, J. B., Watson, W. P., Hunter, W. N., and Brown, T. (1994) *Biochemistry 33*, 10266−10270.
26. Shibutani, S., Takeshita, M., and Grollman, A. P. (1991) *Nature 349*, 431−434.
27. Lowe, L. G., and Guengerich, F. P. (1996) *Biochemistry 35*, 9840−9849.
28. Kamiya, H., Murata-Kamiya, N., Fujimuro, M., Kido, K., Inoue, H., Nishimura, S., Masutani, C., Hanaoka, F., and Ohtsuka, E. (1995) *Jpn. J. Cancer Res. 86*, 270−276.
29. Pinz, K. G., Shibutani, S., and Bogenhagen, D. F. (1995) *J. Biol. Chem. 270*, 9202−9206.
30. Furge, L. L., and Guengerich, F. P. (1998) *Biochemistry 37*, 3567−3574.
31. Miller, H., and Grollman, A. P. (1997) *Biochemistry 36*, 15336−15342.
32. Kerr, S. G., and Anderson, K. S. (1997) *Biochemistry 36*, 14056−14063.
33. Spence, R. A., Anderson, K. S., and Johnson, K. A. (1996) *Biochemistry 35*, 1054−1063.
34. Spence, R. A., Kati, W. M., Anderson, K. S., and Johnson, K. A. (1995) *Science 267*, 988−993.
35. Barshop, B. A., Wrenn, R. F., and Frieden, C. (1983) *Anal. Biochem. 130*, 134−145.
36. Wachsstock, D. H., and Pollard, T. D. (1994) *Biophys. J. 67*, 1260−1273.
37. Frieden, C. (1993) *Trends Biochem. Sci. 18*, 58−60.
38. Zimmerle, C. T., and Frieden, C. (1989) *Biochem. J. 258*, 381−387.
39. Kerr, S. G., and Anderson, K. S. (1997) *Biochemistry 36*, 14064−14070.
40. Wöhrl, B. M., Krebs, R., Thrall, S. H., Le Grice, S. F. J., Scheidig, A. J., and Goody, R. S. (1997) *J. Biol. Chem. 272*, 17581−17587.
41. Kuchta, R. D., Benkovic, P., and Benkovic, S. J. (1988) *Biochemistry 27*, 6716−6725.
42. Eger, B. T., Kuchta, R. D., Carroll, S. S., Benkovic, P. A., Dahlberg, M. E., Joyce, C. M., and Benkovic, S. J. (1991) *Biochemistry 30*, 1441−1448.
43. Patel, S. S., Wong, I., and Johnson, K. A. (1991) *Biochemistry 30*, 511−525.
44. Donlin, M. J., Patel, S. S., and Johnson, K. A. (1991) *Biochemistry 30*, 538−546.
45. Capson, T. L., Peliska, J. A., Kaboord, B. F., Frey, M. W., Lively, C., Dahlberg, M., and Benkovic, S. J. (1992) *Biochemistry 31*, 10984−10994.
46. Miller, H., and Perrino, F. W. (1996) *Biochemistry 35*, 12919−12925.
47. Echols, H., and Goodman, M. F. (1991) *Annu. Rev. Biochem. 60*, 477−511.
48. Johnson, K. A. (1993) *Annu. Rev. Biochem. 62*, 685−713.
49. Suo, Z., and Johnson, K. A. (1998) *J. Biol. Chem. 273*, 27250−27258.

BI982163U